



Cite this: *Soft Matter*, 2024,
20, 2348

Stability, biofunctional, and antimicrobial characteristics of cannabidiol isolate for the design of topical formulations†

Sreejarani Kesavan Pillai, ^a Nazia Hassan Kera, ^{ab} Phumelele Kleyi, ^a
Marinda de Beer, ^a Matin Magwaza^c and Suprakas Sinha Ray ^{*ab}

Cannabidiol (CBD) is a high-value natural compound of *Cannabis Sativa* plant. It is a non-psychoactive phytocannabinoid, attracting significant attention as a multifunctional active ingredient for topical applications. Although it is demonstrated that CBD can be used for specific dermatological ailments, reliable data on functionalities are limited. The present study aimed to investigate the structural stability, biofunctionality, and antimicrobial characteristics of CBD isolate to assist in the design of various topical formulations. The stability of CBD in solid and solubilized states was assessed to establish storage and formulation conditions. The performance of CBD solubilized in organic and aqueous media was evaluated for free radical scavenging, tyrosinase, and collagenase enzyme inhibition, which showed good prospects for the ingredient. The antimicrobial activity of solubilized CBD was evaluated against Gram-negative (*E. coli*, *P. aeruginosa*), Gram-positive bacterial strains (*S. aureus*, *S. epidermidis*, *C. acnes*), and fungal strains (*C. albicans*, *M. furfur*) using agar well diffusion and broth microdilution methods. Due to the presence of surfactants in CBD aqueous solution, it displayed a lack of antimicrobial activity against all the tested microorganisms. CBD solubilized in an organic medium showed no activity against Gram-negative bacterial strains but higher activity against tested Gram-positive bacterial and fungal strains.

Received 30th October 2023,
Accepted 9th February 2024

DOI: 10.1039/d3sm01466e

rsc.li/soft-matter-journal

1 Introduction

Recently, cannabinoids sourced from the Cannabis (*Cannabis Sativa*) plant have emerged as versatile bioactive ingredients in science and medicine. These isolated bioactives include tetrahydrocannabinol (THC), cannabidiol (CBD), cannabichromene (CBC), cannabigerol (CBG), cannabinol (CBN), cannabidivarin (CBDV), among other compounds.¹ Of these compounds, CBD, a major phytocannabinoid, which accounts for up to 40% of the Cannabis plant's extract, has gained traction in the mainstream media for its use in skincare as it is not psychoactive, unlike THC.²

Chemically, CBD is considered to have a tetrahydro biphenyl skeleton: a bicyclic core that represents an adduct formed by the monoterpene, *p*-cymene, and the alkyl resorcinol derivative, olivetol (Fig. 1). It exists as two enantiomers, and (–) CBD is one of the major constituents found in *Cannabis Sativa*.^{3,4} CBD is insoluble in water but soluble in organic solvents such as pentane or hexane. At room temperature, it is a colourless crystalline solid. When exposed to light or heat, CBD can undergo oxidation to form mono- and dimeric hydroquinones and degradation.⁵ In strongly basic media and the presence of air, it is oxidized to a quinone. Under acidic conditions, it cyclizes to THC and other cannabinoids.^{6,7}

CBD has become a popular ingredient that has led many brands to incorporate it into their products, which are often marketed for purported benefits of being anti-inflammatory, analgesic, hydrating, moisturizing, and wrinkle-reducing. The estimated global market for CBD was \$4.6 billion in 2018, with projected sales surpassing \$20 billion in the US alone by 2024.³ In June 2018, highly purified CBD Epidiolex[®], a CBD oil preparation, was approved by the US FDA for the treatment of seizures.⁸ A review article published in 2018 concluded that cannabinoid products can potentially treat various dermatological conditions, including acne vulgaris, allergic contact

^a Centre for Nanostructures and Advanced Materials, DSI-CSIR Nanotechnology Innovation Centre, Council for Scientific and Industrial Research, Pretoria 0001, South Africa. E-mail: rsuprakas@csir.co.za

^b Department of Chemical Sciences, University of Johannesburg, Dronfontein 2028, Johannesburg, South Africa. E-mail: ssinharay@uj.ac.za

^c Tautomer Bioscience Pty Ltd., 260 Cradock Ave, Lyttelton Manor, Centurion, 0157, South Africa

† Electronic supplementary information (ESI) available: The NMR spectrum and data of CBD and the melting point of CBD-IS. See DOI: <https://doi.org/10.1039/d3sm01466e>



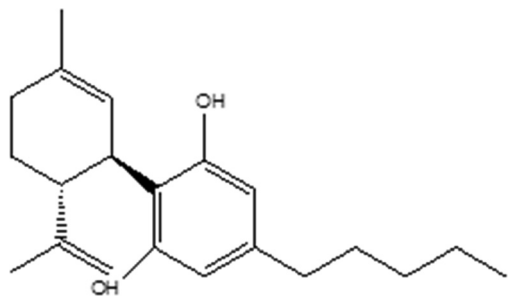


Fig. 1 Chemical structure of CBD.

dermatitis, pruritus, psoriasis, and skin cancer.¹ The cosmetic and dermatological interest in CBD is justified by the fact that CBD can interact with the cutaneous endocannabinoid system, thus bringing various topical visual effects.⁹ This suggests that skin conditions might be affected when CBD molecules bind to these receptors, perhaps by modifying skin cell functionalities such as proliferation, differentiation, and growth.¹⁰ The effects of CBD on the human sebaceous gland were studied on cultured human sebocytes and human skin organ culture, and it was observed that CBD behaves as a highly effective sebo-static agent. CBD is expected to preferentially enter the skin *via* the transfollicular route to accumulate in the sebaceous gland and inhibit the lipogenic actions of various compounds, including arachidonic acid.¹¹ CBD also has been shown to inhibit the proliferation of hyperproliferative keratinocytes.¹²

CBD is presented, in many instances, too enthusiastically as an anti-inflammatory, analgesic, anti-eczema, anti-psoriasis, and anti-itch ingredient.⁴ However, the rapid advances present a unique challenge to the industry and formulators in identifying suitable and demonstrated indications in terms of efficacy and dosage for the responsible use of CBD as an active ingredient in topical product development. Although it is demonstrated that CBD can be used for certain dermatological ailments, reliable data on its safety and efficacy are still limited. CBD is a highly lipophilic molecule; it tends to accumulate within the upper skin layer, the stratum corneum. Effective permeation enhancement strategies must be developed to deliver the activity to the deeper layers of the skin. Another aspect that needs to be attended to is the storage stability of products containing CBD, as it is easily susceptible to structural changes and degradation.⁶ CBD is reported to be an unstable ingredient when exposed to acidic pH, temperature, light, and air.^{13–16} Hence, it is imperative to define the environmental conditions to be used while formulating CBD-based products. Stability studies of the ingredient are essential prior to formulation development to guarantee its proper handling and formulation. The popularity of CBD is increasing, and the plant bioactive is nowadays regarded as the next-generation multifunctional active in skin care, providing a variety of beneficial effects superior to the current commercial ingredients. Together with the identified gaps, these observations demonstrated the critical need for continued research on CBD to

establish its bioactivity or bioavailability due to dosing problems or active ingredient instability in a physiological environment.

This article comprehensively describes the findings from the study on the stability, biofunctional, and antimicrobial characteristics of CBD as an active ingredient for topical applications. A unique combination of characteristics such as high antioxidant, anti-inflammatory, anti-collagenase, antibacterial, and anti-fungal properties is demonstrated for CBD, corroborating its high prospects as a multifunctional ingredient in topical formulations.

2 Experimental

2.1 Materials

Cannabidiol isolate (CBD-IS) [(–)-Cannabidiol, 99.5% purity, ¹H NMR spectrum of the sample is provided in the ESI†], supplied by Tautomer Biosciences Pty Ltd. was sourced from Purisys (Athens, Georgia). Chemicals such as NaOH (ACS reagent grade, ≥97.0 purity, pellets), citric acid (ACS reagent grade, ≥99.5 purity), ethanol (absolute reagent, ≥99.8%), DMSO (extrapure AR, 99.5%) polysorbate 20, 80, eumulgin® CO 40, and eumulgin® O 10 Flex, were sourced from various suppliers (Sigma Aldrich, BASF, South Africa and SRL chemicals India.). De-ionized water (DI water) was used for various preparations where water was required.

2.2 Methods

2.2.1 CBD-IS powder characterization. Thermogravimetric analysis of CBD-IS powder sample (approximately 3.5 mg) in air atmosphere was performed using a thermogravimetric analyzer (TA instruments, model Q550, USA). The temperature was ramped at 10 °C min^{−1} in air, from 25 °C to 300 °C. The thermal stability of the sample was also investigated using high-speed differential scanning calorimetry (DSC) (PerkinElmer Hyper, model Pyris 8500, USA). The temperature was ramped at 10 °C min^{−1} in air, from 25 °C to 200 °C. The sample weights were maintained at a low level (2.90–3.20 mg) to avoid thermal lag. The melting point of the CBD-IS powder sample was determined by a Buchi Melting Point M-565 instrument (Buchi, USA). X-ray diffraction (XRD) studies were conducted using an X'Pert PRO X-ray diffractometer (PANalytical, Netherlands) operating with Cu K-α radiation (wavelength of 0.15406 nm) at 45 kV and 40 mA. The exposure time and scan speed for the XRD measurements were 19.7 min and 0.036987° s^{−1}, respectively. The vibrational characteristics of CBD-IS were followed by Fourier transform infrared (FTIR) spectroscopy (PerkinElmer Spectrum 100 spectrometer, USA) with the MIRacle ATR attachment and a Zn/Se plate. A small amount of sample was pressed onto the Zn/Se plate, and spectra over the range of 550 to 4000 cm^{−1} were collected.

2.2.2 CBD-IS solubilization. The solubility of 1 g of CBD-IS powder in 5 mL ethanol and 5 mL DMSO was confirmed. The solutions were further diluted with respective solvents, and 1000 ppm concentration was analyzed with a UV-Vis



spectrophotometer (PerkinElmer Lambda 750s, USA) using the corresponding solvents as blank. The solubilization capability of surfactants with different hydrophilic-lipophilic balance (HLB) such as polysorbate 20, 80, eumulgin[®] CO 40, and eumulgin[®] O 10 Flex was established by preparing a mixture containing 1 g CBD-IS powder, 9 g of surfactant and 90 g of DI water. The optimal solution was selected, diluted further with DI water to 1000 ppm, and analyzed with a UV-Vis spectrophotometer (PerkinElmer Lambda 750s, USA) using the corresponding surfactant water mixture as blank. The ethanolic and surfactant solutions of CBD-IS were designated as CBD-IS-E and CBD-W, respectively.

2.2.3 pH stability of solubilized CBD. The structural stability of CBD-IS-E and CBD-W (1000 ppm) was investigated for any possible structural variations under different conditions of pH (4, 5, 6, 7, 9) to find the optimum formulation pH. Before and after pH adjustment, the CBD mixtures were subjected to UV-Vis spectroscopy (PerkinElmer Lambda 750s, USA) for quantitative analyses. For the CBD-IS-E solution, the pH was adjusted by using 18% ethanolic NaOH and 50% citric acid. The pH was adjusted for the CBD-W solution using 18% NaOH and 50% citric acid. Data are the average value of duplicates and expressed as mean \pm SD.

2.2.4 Temperature stability of solubilized CBD. The structural stability of CBD-IS-E and CBD-W (1000 ppm) were investigated for any possible structural variations under different conditions of temperature (3 °C, 25 °C, 37 °C, and 50 °C) for 24 h to find the optimum formulation processing temperature. The concentration before and after exposure to various temperatures was determined by UV-Vis spectroscopy (PerkinElmer Lambda 750s, USA) for quantitative analyses. Data are the average value of duplicates and expressed as mean \pm SD.

2.2.5 DPPH antioxidant assay. The 1,1-diphenyl-2-picrylhydrazyl (DPPH) oxidative assay was followed as described by Mavundza *et al.*¹⁷ with slight modifications. The final concentration of the samples (CBD-IS-E and CBD-W) ranged between 500 to 0.08 $\mu\text{g mL}^{-1}$, and for the positive control, L-ascorbic acid (vitamin C) between 100 $\mu\text{g mL}^{-1}$ to 0.78 $\mu\text{g mL}^{-1}$ in 100% ethanol. To each of the wells, 90 μM DPPH ethanolic solution was added and left to incubate in the dark for 30 min at room temperature. Ethanol (100%) was included as a blank. The extracts' radical scavenging capacities were determined using a multi-well plate reader (BIO-TEK Power Wave A.D.P., Weltevreden Park, South Africa) at 515 nm. The results were expressed as the average effective concentration (EC_{50}) of the sample to reduce the initial absorbance of the DPPH radical by 50%.

2.2.6 Anti-tyrosinase activity. The method used to determine tyrosinase inhibition was followed as described by Lall *et al.*¹⁸ with moderate alterations. Kojic acid at 20 mg mL^{-1} served as the positive control, with the final concentration ranging from 120–0.94 $\mu\text{g mL}^{-1}$. The assay was conducted in a working solution of potassium phosphate buffer (pH 6.5), tyrosinase enzyme (333 units per mL in phosphate buffer) and 44 mg mL^{-1} L-tyrosine substrate. A vehicle control containing 2% DMSO and two negative controls (one in which no enzyme

was added and the other in which no substrate was added). The samples were incubated for 5 min with the tyrosinase enzyme, and after incubation, the substrate was added. Therefore, the final concentration range of the sample was 504–3.94 $\mu\text{g mL}^{-1}$. Using a microplate reader (BIO-TEK Power-Wave XS, Analytical and Diagnostic Products CC, South Africa), the absorbance values were determined at a wavelength of 292 nm for 30 minutes immediately following the addition of the substrate. The percentage inhibition was calculated using the following equation:

$$\% \text{ inhibition} = 100 - \left(\frac{\text{Absorbance sample}}{\text{Absorbance control}} \right) \times 100$$

where 'absorbance control' is the (absorbance of DMSO at time 30) – (absorbance of DMSO at time 0); 'absorbance sample' is the (absorbance of the extract or positive control at time 30) – (absorbance of the sample or positive control at time 0). The EC_{50} values were calculated for values where 50% inhibition was observed.

2.2.7 Anti-collagenase property. The anti-collagenase activities of the samples were studied to determine their potential anti-aging properties. Collagenase assays were carried out according to previously reported methods in the literature that were modified accordingly.^{19,20} In this assay, the production of coloured fragments arising from the cleaving of collagenase chromophore-substrate by collagenase enzyme was monitored spectrophotometrically. Collagenase from *Clostridium histolyticum* was dissolved in 20 mM CaCl_2 solution. The collagenase chromophore-substrate was dissolved in 0.2 mL methanol and diluted with Tris-HCl buffer (100 mM, pH 7.1) to a final concentration of 0.1 mM. CBD-IS-E stock solution was prepared in 10% (v/v) ethanol. CBD-IS-E and CBD-W solutions were serially diluted in Tris-HCl buffer (100 mM, pH 7.1). For the assay, 0.6 mL aliquots of CBD-IS-E and CBD-W sample solutions (125–2000 $\mu\text{g mL}^{-1}$) were incubated with 0.1 mL aliquots of enzyme solution (2 mg mL^{-1}) and 0.3 mL of Tris-HCl buffer (100 mM, pH 7.1) for 10 min at room temperature. For the control, 100 μL of the enzyme solution was incubated with 900 μL of Tris-HCl buffer (100 mM, pH 7.1) as for the sample solutions. Aliquots of collagenase chromophore-substrate solution (2 mL, 0.1 mM) were added to the control and test samples to start the reactions, and the mixtures were incubated at 37 °C for 30 min. Aliquots of citric acid (1 mL, 25 mM) were then added to the mixtures to terminate the reactions. Ethyl acetate (5 mL) was added to the mixtures, which were then shaken vigorously for 15 seconds for extraction of the coloured fragments. Once the mixtures had settled, the ethyl acetate fraction was carefully transferred into tubes containing 300 mg of Na_2SO_4 . The tubes were then shaken, and the ethyl acetate extract was filtered through Whatman filter paper. The absorbances of the ethyl acetate filtrate were measured at 320 nm using a UV-Vis spectrometer (PerkinElmer Lambda 750s, USA). EDTA was used as a positive control. The EC_{50} values were calculated for values where 50% inhibition was observed.



2.3 Microbiological assays

2.3.1 Culturing of test microorganisms. The Gram-negative (*E. coli*) and Gram-positive bacteria (*S. aureus* and *S. epidermidis*) were pre-cultured in nutrient broth overnight in a rotary shaker at 37 °C. *P. aeruginosa* was pre-cultured in nutrient broth for 48 h and *C. acnes* was pre-cultured under anaerobic conditions in trypticase soy broth (TSB) overnight. Thereafter, each strain was adjusted at a concentration of approximately 1.5×10^8 CFU mL⁻¹ using a 0.5 McFarland standard. The *C. albicans* inoculum was prepared from the 48 h culture of fungal isolates in potato dextrose broth (PDB). The *M. furfur* inoculum was prepared from the 48–72 h culture of fungal isolates in PDB containing 2% olive oil.

2.3.2 Antimicrobial activity evaluation – agar well diffusion method. The agar well diffusion method was used to evaluate the antibacterial and anti-fungal activities of two different CBD solutions (CBD-IS-D where DMSO was used as the solvent) and CBD-W). Firstly, 100 µL of fresh bacterial or fungal culture was pipetted and spread on agar plates. Wells were bored using a sterile micropipette tip into agar plates containing inoculums. Then, 150 µL of each CBD solution was added to the respective wells. The plates were incubated at 37 °C for 18 h and the antimicrobial activity was detected by measuring the zone of inhibition (including the diameter of the well) that appeared during the incubation period. Pure DMSO was used as a negative control as it was used for the dissolution of CBD-IS. All experiments were done in triplicates.

2.3.3 Antimicrobial activity evaluation – broth microdilution method. The test microorganisms from the stock cultures were inoculated in appropriate broth media and incubated at 37 °C under stirring for 2–24 h until an optical density (OD) between 0.6 and 0.8 at 625 nm was reached. The CBD-IS-D solution (0.625 mg mL⁻¹) was serially diluted using 96-well microplates in a final volume of 200 µL. In each dilution, 50 µL of microbial suspension (approximately 1.5×10^6 CFU mL⁻¹). The microplates were covered with sterile lids, sealed with a parafilm, and agitated to mix the contents of the wells by using a rotary shaker. Then, the plates were incubated at 37 °C for 24–72 h.

3 Results and discussion

3.1 Stability aspects of CBD-IS

3.1.1 CBD-IS powder characterization. Four characterization techniques, namely, TGA, DSC, XRD, and FT-IR, were used on the as-received CBD-IS powder sample to assess the thermal stability, crystallinity, and functional groups in CBD.

The TGA thermogram of the CBD-IS powder sample is presented in Fig. 2(a). A single-step thermal degradation is observed for CBD. The TGA analysis shows that CBD-IS is stable up to 100 °C, and the decomposition starts after 150 °C. This indicates the stability of the CBD powder at room temperature storage conditions. Fig. 2(b) reports a DSC thermogram with an endotherm around 68.7 °C, which could be due to ($\Delta H_{\text{vap}} = 62 \text{ J g}^{-1}$) the melting of CBD-IS as many organic compounds melt before undergoing decomposition.²¹ If it represented a

physisorbed water loss event, it should have been observed in the TGA thermogram through mass loss, but the mass remains constant until decomposition begins. The initiation of degradation was observed above 140 °C, which is in line with the TGA observations. The DSC endothermic peak at 68.97 °C for CBD-IS was also observed by Andriotis *et al.*²¹ and Vlad *et al.*²² According to the authors, CBD-IS decomposition might occur at temperatures higher than 300 °C. The melting of CBD-IS powder was measured to be 68.6 ± 0.2 °C which substantiated the TGA and DSC observations. The XRD spectrum (Fig. 2(c)) shows sharp crystalline peaks for CBD. The 2θ angle values characteristic for CBD are 9.66°, 10.24°, 11.78°, 12.53°, 13.08°, 15.34°, 19.85°, 19.03°, 21.66°, 22.73°, 23.79°, 25.29°, 26.42°, 29.19° with the highest intensity occurring in the case of 9.66°.²³ Lv *et al.*²⁴ reported similar observations on the XRD pattern of pure crystalline CBD. Fig. 2(d) displays an FT-IR spectrum of the CBD-IS powder sample. The FTIR spectrum shows all the characteristic peaks (Table 1) for the functional groups in CBD-IS, which agree with the previous reports.^{25,26}

The stability profile of CBD-IS powder from TGA and DSC shows that the integrity of the sample is maintained in powder form up to 65 °C, and low temperature is not necessary for its storage. Kosovic *et al.*²⁷ observed better stability of CBD powder when compared to CBD dissolved in sunflower oil. According to the study, the integrity of the CBD in powder form exposed to 25 °C/60% RH remained unchanged for 270 days.

4.1.2 CBD-IS solubilization. The solubility of CBD-IS powder in different organic solvents (ethanol, DMSO) and its solubilization in various surfactant/water mixtures were tested. CBD-IS was readily soluble in the tested organic solvents. Generally, cannabinoids are negligibly soluble in water but are highly soluble in lipids and accumulate abundantly in the body's fatty tissues.²⁴ Solubilizers (surfactants) were required to improve the aqueous solubility of CBD due to the hydrophobic nature of CBD. Of the different surfactant mixtures tested, polysorbate 20 with an HLB of 16.7 showed better results. Although polysorbate 80 (HLB 15), eumulgin® CO 40 (HLB 14), and eumulgin® O 10 Flex (HLB 15) were effective in solubilizing CBD, the mixtures were more turbid in comparison to the surfactant mixture of polysorbate 20. The micellar solubilization of CBD was found to be dependent on the HLB of the surfactants,²⁸ and the study demonstrated increased solubility of CBD-IS in polysorbate,²⁰ which could enhance the bioavailability of poorly water-soluble CBD-IS in emulsion formulations. The UV-Vis spectra of solubilized CBD-IS at a concentration of 1000 ppm in ethanol (CBD-IS-E) and polysorbate 20/water mixture (CBD-W) are presented in Fig. 3(a) and (b).

Fig. 3(a) and (b) indicate that CBD-IS exhibits strong absorption peaks at 274 and 280 nm within the ultraviolet region. In fact, CBD-IS shows two poorly separated maxima at 274 and 280 nm. According to Schmidt *et al.*,²⁹ the completely protonated neutral form of CBD exists below the pK_a values. In the case of CBD, no experimental pK_a values are available in the literature. Still, it is envisaged that they could be > 9 , based on a comparison with the core structure resorcinol ($pK_a = 9.32^{30}$).



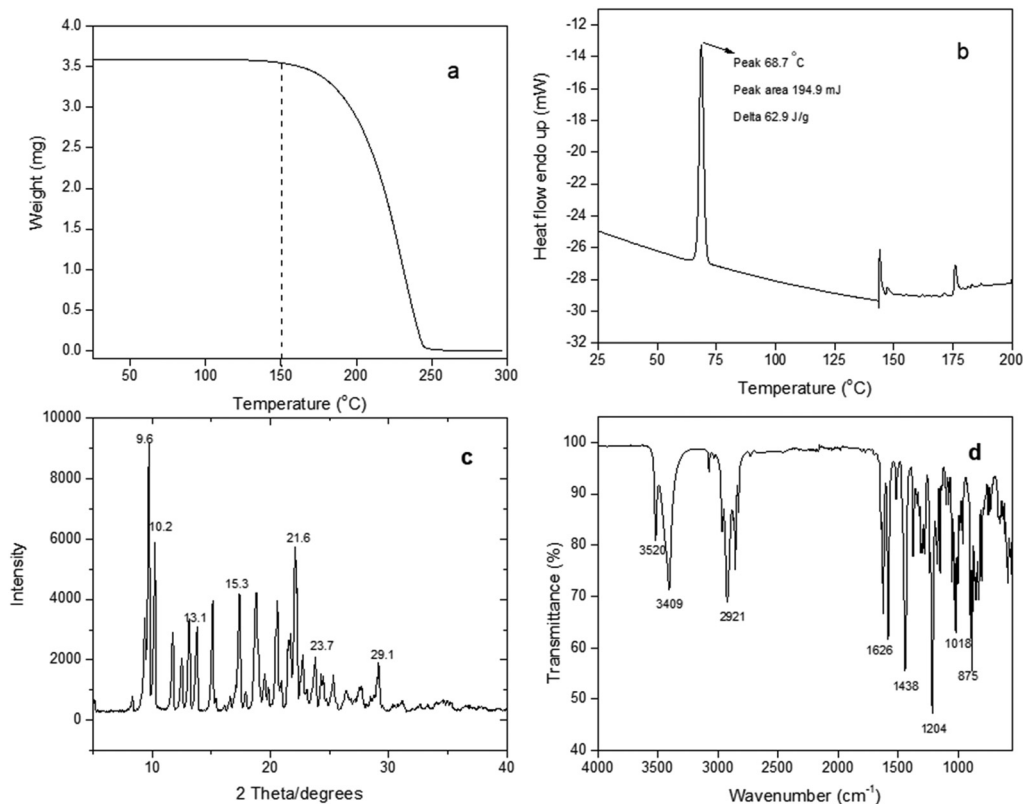


Fig. 2 (a) TGA thermogram, (b) DSC thermogram, (c) XRD pattern, and (d) FTIR spectrum of CBD-IS powder.

Table 1 FT-IR characteristic peak positions and assignment of functional groups associated with CBD-IS powder

Wavenumber (cm ⁻¹)	Group – bond	Functional group
3409	O–H stretch	Alcohols/phenols
2921	C–H stretch	Alkane
1626	C=C stretch	Alkene
1438	C–H bend, rock	Alkane
1204	C–H wag	Alkane
1019	C–O stretch	Esters/ethers/carboxylic acids/alcohols
875	C–H bend	Alkene

The pH of ethanolic and surfactant-based forms of CBD was measured to be 6.6 and 5.6, respectively. The pH values below pK_a ensure that only the neutral form exists. The absorption band at 280 nm is characteristic of the phenolic core structure and shows the HOMO–LUMO $\pi \rightarrow \pi^*$ transition.³¹

4.1.3 pH stability of solubilized CBD. The ethanolic and surfactant-based solutions of CBD-IS were prepared (CBD-IS-E and CBD-W, respectively), and the pH of the original solutions without any pH adjustments was measured as 6.6 and 5.6, respectively. The solutions were divided into different portions of 25 mL, and the pH was adjusted to the values reported in Table 2.

The CBD-IS-E sample was not significantly affected by the changes in the pH, as the absorption values did not change, indicating the CBD is stable under the experimental conditions

(Fig. 4(a)). However, CBD-W showed destabilization at pH values below and above 7, as evident from the lower absorbance values obtained (Fig. 4(b)). The CBD-W also showed purple colouration at high pH in a basic medium. The observed decrease in CBD concentration and colour change could be due to structural changes. Cannabidiol undergoes chemical transformations when the pH is changed. Under acidic conditions, it may transform into Δ^9 -THC by acid-catalyzed cyclization,³² and under basic conditions, in the presence of oxygen, it is oxidized to monomeric and dimeric hydroxyquinones. A characteristic sign of such transformation is a colour change of the solution where a purple colour is produced due to the accumulation of the anions of hydroxyquinone and its dimer.³³ Fraguas-Sanchez and co-workers³⁴ also showed that CBD is more stable in ethanol than in aqueous solvents, with a t_{95} value of 7 days at 25 °C when water with 0.5% polysorbate 80 was used as a surfactant. This instability was partly attributed to dissolved oxygen, which is more reactive than atmospheric oxygen.

The experimental results indicated a clear difference between the CBD content of the aqueous form depending on pH conditions, whereas ethanol provided stable CBD solutions. The solvent influences CBD stability, which is more stable in ethanol than in an aqueous medium. The results suggest the importance of maintaining a neutral pH condition for CBD in an aqueous medium. The instability of CBD in an aqueous medium should be considered when such medium-based



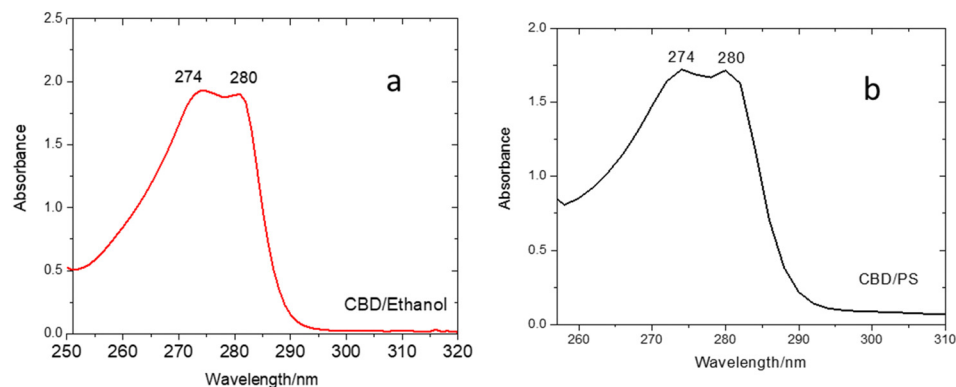


Fig. 3 UV-Vis spectrum of (a) CBD-IS-E and (b) CBD-W.

Table 2 pH of CBD solutions before and after pH adjustment

	pH				
	Original	1	2	3	4
CBD-IS-E	6.6	3.6	4.8	5.9	9.0
CBD-W	5.6	4.4	5.6	6.8	9.0

in vitro and *in vivo* studies of CBD are conducted (freshly prepared samples should be used) and in the development of various product forms.

4.1.4 Temperature stability of solubilized CBD. Single batches of CBD-IS-E and CBD-W were prepared, and the solutions were divided into different portions of 25 mL and exposed to different conditions of temperature (3 °C, 25 °C, 37 °C, and 50 °C) for 24 h to find the optimum formulation processing temperature conditions. The absorbance values obtained for CBD-IS-E and CBD-W are presented in Fig. 5(a) and (b), respectively.

The CBD-IS-E was not greatly affected by the changes in the temperature. The slight increase in absorbance at higher temperatures could be accounted for by the increase in CBD concentration as ethanol evaporated. However, CBD-W, on the other hand, showed destabilization with an increase in

temperature. The highest stability for CBD-W was observed for the solution stored at 3 °C. Although discolouration was not observed, the decrease in absorption values indicated a structural change in the aqueous form in the presence of a surfactant. Fraguas-Sanchez *et al.*³⁴ reported lower stability of aqueous solutions of CBD when compared to ethanolic solutions. They observed 10% degradation for CBD in simulated physiological conditions (pH 7.4 and 37 °C) within 24 h.

Another observation was a slight change in colour to a darker yellow in the case of the ethanolic samples stored at room temperature but not in the dark after 4 days of storage. A change of colour of the solution from colourless to light yellow and dark yellow with time indicates the processes of oxidation, polymerization, and other chemical changes.³⁵ Fairbairn *et al.*³⁶ showed that light-exposed samples stored in various solvents degraded faster than samples stored in the same solvents in the dark, while Turner and Hanry³⁷ reported that THC and CBD either in solution or in crude extract form were stable for six days when exposed to both natural and artificial light which is contrary to the observations in this study. According to the authors, exposure to light alone for a given time does not lead to significant changes in the CBD content. Still, in combination with other factors, such as the solvent

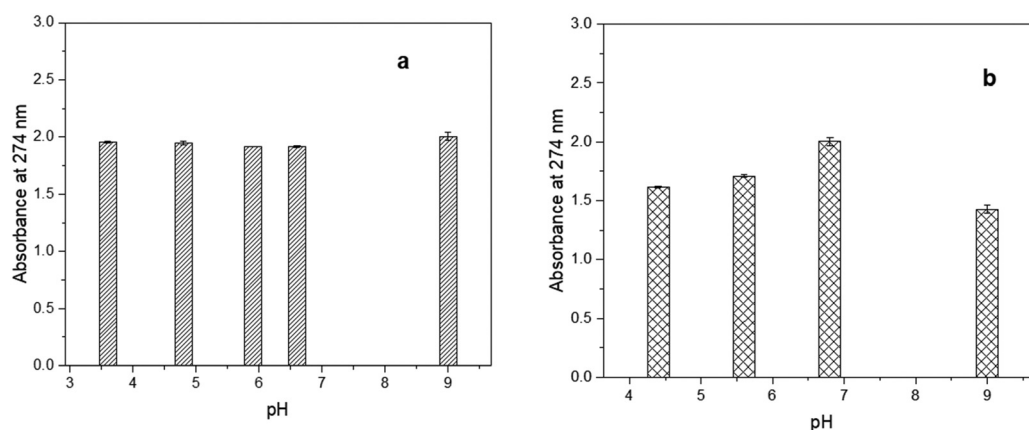


Fig. 4 UV-Vis spectrum of CBD-IS exposed to different pH conditions at 25 °C (a) CBD-IS-E and (b) CBD-W.



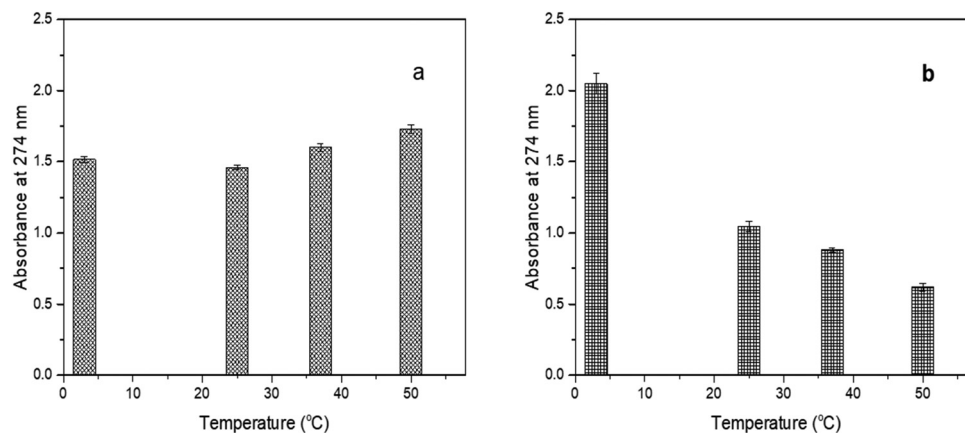


Fig. 5 UV-Vis spectrum of CBD-IS exposed to different temperature conditions (a) CBD-IS-E and (b) CBD-W.

used, increased temperature, and the presence of oxygen, light may accelerate the degradation process, which in our case might be due to oxidation of CBD in the presence of light and oxygen. Solvents have been shown to affect CBD's stability significantly. In this study, ethanol yielded more pH and temperature-stable solutions of CBD in comparison to CBD in an aqueous solution. However, due to high lipophilicity, CBD might precipitate in the emulsion formulation, which can affect the efficacy and stability of products.³⁸ Surfactants such as polysorbate 20 could improve their solubilization through micelle formation, where the surfactant molecules arrange themselves on the surface of the spherical oil droplets with the surfactant nonpolar heads entrenched into the oil droplet and the polar head into the aqueous phase. This situation ensures minimal or no interaction between the active ingredient (*e.g.*, CBD) and the other chemical ingredients in the formulation, such as waxes, surfactants (emulsifiers), oils, rheology modifiers, and water.³⁹ Thus, the most probable parameters that can affect the stability of CBD in the formulation are pH, temperature, as well as external environmental factors (frequency of light radiation, oxidation, humidity *etc.*) as previously mentioned in this section. Yet, events of destabilizing interactions of plant bioactive⁴⁰ like CBD with emulsifiers (dilution effect),⁴¹ rheology modifiers (decrease in viscosity),⁴² and surfactants (increase in droplet sizes)⁴³ are possible during its incorporation into formulations.

4.2 Biological functionalities of CBD

4.2.1 DPPH antioxidant assay. 1,1-Diphenyl-2-picrylhydrazyl (DPPH) is a stable organic radical with an unpaired electron at one atom of its nitrogen bridge. DPPH can be used to detect antioxidants through the DPPH oxidative assay. The assay is based on the capacity of the biological reagent to scavenge the radical DPPH and is expressed as the magnitude of antioxidant ability. The DPPH alcohol solution is deep purple and absorbs at 515 nm. In the presence of a free radical scavenger, the purple colour is reduced to a more yellow hue as the unpaired nitrogen electron in DPPH is paired.⁴⁴ The EC_{50} values (concentrations of samples able to reduce the initial absorbance of

DPPH radicals by 50%) obtained for CBD-IS-E, CBD-W, and positive control ascorbic acid are presented in Table 3.

The positive control *L*-ascorbic acid scavenged 50% of the free radicals at a concentration (EC_{50}) of $3.25 \pm 0.91 \mu\text{g mL}^{-1}$. The EC_{50} value for the DPPH radical scavenging activity of sample CBD-IS was $2.02 \pm 0.34 \mu\text{g mL}^{-1}$, which was very similar to the positive control (Table 3 and Fig. 6). From the results, it is apparent that both ethanolic and aqueous solutions of CBD have antioxidant properties. CBD-IS-E showed excellent antioxidant activity in comparison to CBD-W. The lower antioxidant property of CBD-W could be due to the presence of surfactants in the reaction mixture where CBD is solubilized in a micelle and less accessible to DPPH molecules. Kitamura *et al.*⁴⁵ performed DPPH assays on CBD oil samples and obtained EC_{50} values 522 to 1075 μM (164 to $338 \mu\text{g mL}^{-1}$). Russo *et al.*⁴⁶ also observed EC_{50} values around 3180 μM ($1000 \mu\text{g mL}^{-1}$), much higher than the values obtained in this study. A study by Tura *et al.*⁴⁷ determined that CBD has the potential to neutralize free radicals, thus serving as an antioxidant. The results from this study also agree with the observations by Hampson *et al.*⁴⁸ suggesting that CBD had similar antioxidant potential compared to the antioxidant butylated hydroxytoluene (BHT), and CBD had a superior antioxidant effect than other dietary antioxidants, α -tocopherol or ascorbate. Previous studies suggest formal hydrogen transfer and radical adduct formation as the main radical scavenging mechanisms for CBD.⁴⁹ While both are single-step mechanisms, the former involves a direct transfer of a hydrogen atom from CBD to the free radical. In contrast, in the latter case, free radicals could be stabilized by resonance over the ether and alkyl groups and on the benzene ring of CBD.⁵⁰ The mechanisms of antiradical activity of CBD could be like that of established antioxidants such as ascorbic

Table 3 DPPH free radical scavenging activity of samples

Sample	$EC_{50} \pm \text{SD} (\mu\text{g mL}^{-1})$
CBD-IS-E	2.02 ± 0.34
CBD-W	126.69 ± 3.23
<i>L</i> -Ascorbic acid	3.25 ± 0.91



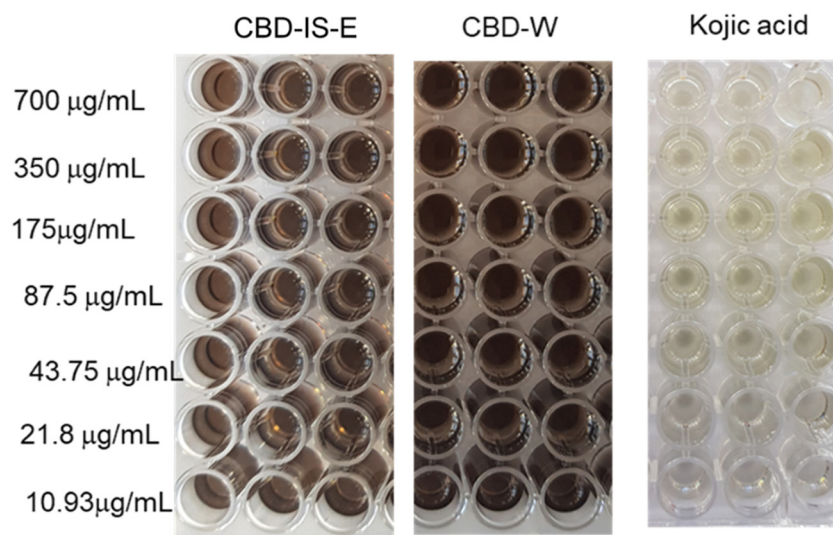


Fig. 6 Representation of microplates of tyrosinase assay for CBD-IS-E and CBD-W.

acid, where the antioxidant functionality is based on formal hydrogen transfer, quenching of singlet oxygen, and removal of molecular oxygen.⁵¹

4.2.2 Anti-tyrosinase activity. Over the years, various plant bioactives have been used to reduce tyrosinase activity, whose function is to catalyze two reactions within a process known as melanogenesis. These include the hydroxylation of tyrosine to 3,4-dihydroxyphenylalanine (DOPA) and the oxidation of DOPA to dopaquinone.^{52,53} Afterwards, dopaquinone undergoes a series of reactions, producing either pheomelanins (light pigment) or eumelanins (dark pigments). Overstimulation of tyrosinase production causes a phenomenon known as hyperpigmentation, while the underproduction of this catalyst results in hypopigmentation.⁵³ The results obtained for anti-tyrosinase activity for CBD-IS-E and CBD-W samples are presented in Fig. 6.

The colour difference between positive control and CBD samples indicated anti-tyrosinase activity only for kojic acid. Kojic acid (positive control) displayed an average EC_{50} of $3.27 \pm 0.19 \mu\text{g mL}^{-1}$. None of the tested CBD samples showed an inhibition effect on the tyrosinase activity. No anti-tyrosinase activity was observed for CBD samples at the tested concentrations of up to $700 \mu\text{g mL}^{-1}$. In fact, an increased tyrosinase activity was observed at higher concentrations of CBD, *i.e.*, 350 and $700 \mu\text{g mL}^{-1}$. Manosroi *et al.*⁵⁴ reported anti-tyrosinase activity for hemp leaf extract with an EC_{50} value of $48 \pm 0.02 \mu\text{g mL}^{-1}$ which exhibited more potent tyrosinase inhibition activity than the hemp seed extract (EC_{50} value of $70 \pm 0.06 \mu\text{g mL}^{-1}$) but displayed lower activity than kojic acid (EC_{50} value of $5 \pm 0.004 \mu\text{g mL}^{-1}$) by 9.8 and 14 times, respectively. In a recent article, Goenka⁵⁵ reported that CBD stimulated melanin synthesis in HEMn-LP cells in a concentration-dependent manner. The increase in melanin synthesis due to the tyrosinase inhibition activity of CBD at $2 \mu\text{M}$ was significantly higher by 21.53% than at $1 \mu\text{M}$. In another study, Hwang and co-workers⁵⁶ reported that CBD

increases tyrosinase activity and melanin content mediated by the CB1 receptors in human epidermal melanocytes. Despite not exhibiting anti-tyrosinase activity, CBD's superior antioxidant properties could play a role in decreasing hyperpigmentation and melanogenesis caused by UV rays.⁵⁷

4.2.3 Anti-collagenase activity. Collagenase is an enzyme in the matrix metalloproteinase (MMP) family that breaks down collagen, assisting in the degradation of the extracellular matrix and leading to skin ageing. Collagenase can cleave collagen or similar substrates through hydrolysis. Any materials that preferentially block the binding sites of collagenase will inhibit its activity and hence have anti-collagenase properties.⁵⁸ The ability of an active to inhibit collagenase was determined by measuring the release of coloured breakdown product spectrophotometrically. The EC_{50} values obtained for CBD samples are presented in Fig. 7.

The effect of CBD-IS-E and CBD-W on collagenase activity is shown in Fig. 7. CBD-IS-E reduced collagenase activity at concentrations of $100 \mu\text{g mL}^{-1}$ and above, where collagenase inhibition increased with CBD-IS-E concentration. CBD-W inhibited collagenase activity when present at a concentration of $200 \mu\text{g mL}^{-1}$, indicating that at least twice the concentration of CBD-W was required to inhibit the enzyme activity. The EC_{50} values for CBD-IS-E and CBD-W were calculated to be 311.1 and $624.2 \mu\text{g mL}^{-1}$, respectively. The positive control EDTA effectively inhibited elastase activity; the EC_{50} calculated was $67.2 \mu\text{g mL}^{-1}$. Zagórska-Dziok *et al.*⁵⁹ found that hemp extracts decreased the activity of collagenase in a concentration-dependent manner. At a concentration of $250 \mu\text{g mL}^{-1}$, the extract showed the ability to reduce collagenase activity by 30%. At $1000 \mu\text{g mL}^{-1}$, the value of the analyzed parameter was up to 80%. Gegotek and co-workers⁶⁰ reported the inhibitory role of CBD on MMP secretion and activity in the blood plasma and keratinocytes isolated from psoriatic patients using the quantitative chemiluminescent method of detection based on an ELISA protocol and zymography technique. It was shown that



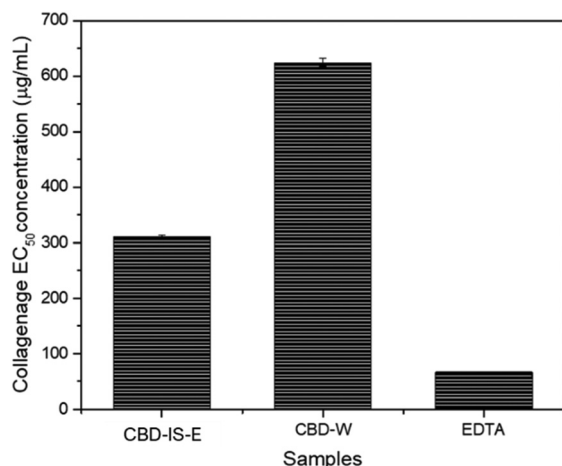


Fig. 7 Collagenase inhibition activity of CBD-IS-E and CB-W.

CBD caused a significant reduction of the activity levels of all assessed MMPs (MMP-1/2/3/7), indicating its antiangiogenic properties. While Ramer *et al.*⁶¹ highlighted the anti-invasive action of CBD through the downregulation of MMPs in human cervical cancer (HeLa, C33A) and human lung cancer cells (A549), Rawal and colleagues⁶² reported the MMP inhibitory effect of CBD on human gingival fibroblast which are in line with the collagenase inhibition property of CBD observed in this study.

4.3 Antimicrobial properties of CBD

4.3.1 Agar well diffusion method. Two solutions of CBD (0.625 mg mL⁻¹), one dissolved in DMSO (CBD-IS-D), and the other, a surfactant/water dispersion (CBD-W), were evaluated for potential antimicrobial activity against Gram-negative (*E. coli*, *P. aeruginosa*), Gram-positive (*S. aureus*, *S. epidermidis*, *C. acnes*) bacterial strains, as well as fungal strains *C. albicans* and *M. Furfur*. The agar well diffusion method revealed that CBD-IS-D displayed no antimicrobial activity against Gram-negative bacterial strains (*E. coli*, *P. aeruginosa*) (Fig. 8(a) and (b)). However, it exhibited excellent antimicrobial activity against the Gram-positive *C. acnes* – the skin acne-causing bacteria (Fig. 8(c)). For the Gram-positive bacterial strains, CBD-IS-D exhibited moderate activity against *S. aureus* (Fig. 8(d)), while the activity against *S. epidermidis* was excellent (Fig. 8(e)). There was also some significant antimicrobial activity against *C. albicans* by CBD-IS-D (Fig. 8(f)). CBD-W did not exhibit any antimicrobial activity against all the microorganisms (Gram-negative, Gram-positive bacterial strains, and the fungal yeast strain (Fig. 8(g)–(i)). This general lack of antimicrobial activity can partly be attributed to the presence of surfactants that can interfere with the direct interaction of CBD molecules with the microbial surface. There appears to be a common observation regarding the antimicrobial efficacy of CBD against some Gram-negative and Gram-positive bacterial strains.⁴⁹ As with our observations, previous reports reveal that CBD displayed good antimicrobial activity against *S. aureus*.⁶³

In contrast, moderate or no activity was observed for *E. coli*, *P. aeruginosa* and *C. albicans*.^{64,65} Generally, aqueous, acetic, ethanolic, methanolic, and petroleum ether extracts of CBD have been used. While generally inactive against Gram-negative bacterial strains, CBD has interestingly been reported to preferentially inhibit the growth of a small subset of Gram-negative bacterial strains, including *Neisseria gonorrhoeae*.⁶⁶ According to Blaskovich *et al.*,⁶⁶ CBD induced membrane permeabilization by acting quickly to disrupt bacterial cytoplasmic membranes in Gram-positive bacteria and inhibiting the protein, DNA, RNA and peptidoglycan synthesis pathways. On the other hand, the limited activity of CBD against Gram-negative bacteria could be due to the outer peptidoglycan cell wall surrounded by a lipopolysaccharide membrane. Wassman and co-workers⁶⁷ also showed that the combination of CBD with the antibiotic Bacitracin selectively inhibited various Gram-positive bacterial strains while not showing activity against Gram-negative bacteria. The authors observed many septa formations during the cell division together with cell membrane irregularities on morphological evaluation. The excellent antimicrobial activity against *C. acnes* and *S. epidermidis* opens a great opportunity for CBD to be an active ingredient in cosmetic formulations for anti-acne functionality. Due to inconsistent growth on agar plates, the agar well diffusion method could not be applied to *M. furfur* – a fungal strain associated with dandruff.

The microorganisms that displayed susceptibility to CBD-IS-D were selected for the microdilution experiments to determine the minimum inhibitory concentration (MIC). Moreover, due to its inconsistent growth on agar, *M. furfur* was included in microdilution dilution experiments.

4.3.2 Broth microdilution method. The minimum inhibitory concentration (MIC) for CBD-IS to inhibit the growth of the selected microorganisms (*S. aureus*, *S. epidermidis*, *C. acnes*, *C. albicans*) with a positive response in the well-diffusion assay was determined using the microdilution method. Table 4 presents the determined MICs for CBD-IS-D for various bacterial and fungal strains. The MICs agree with the agar well diffusion results that CBD-IS-D exhibits more antibacterial (against Gram-positive bacterial strains) than the fungal strains. CBD-IS-D attained the lowest MIC (2.44 µg mL⁻¹) against Gram-positive bacterial strains (*S. epidermidis*, *C. acnes*). However, the MIC for CBD-IS-D against *S. aureus* was 64 times (156.25 µg mL⁻¹) higher than that of the other Gram-positive strains. CBD-IS-D attained relatively higher MICs for both fungal strains, *C. albicans* (>312.5 µg mL⁻¹) and *M. furfur* (312.5 µg mL⁻¹).

The MIC value of CBD-IS-D against *S. aureus* is within the range of MIC (1–1000 µg mL⁻¹) values reported by other researchers.^{68,69} The observed MIC value of 2.44 µg mL⁻¹ for CBD-IS against *S. epidermidis* is comparable to the value in the literature (4 µg mL⁻¹).⁶⁵ The observed MIC values for CBD-IS against *C. albicans* and *M. furfur* were 25 times higher than the literature-reported MIC value (12.46 µg mL⁻¹).⁷⁰ This could mean that in practical formulation, the targeted microbe, its concentration, and the dosage rate of CBD could be the crucial



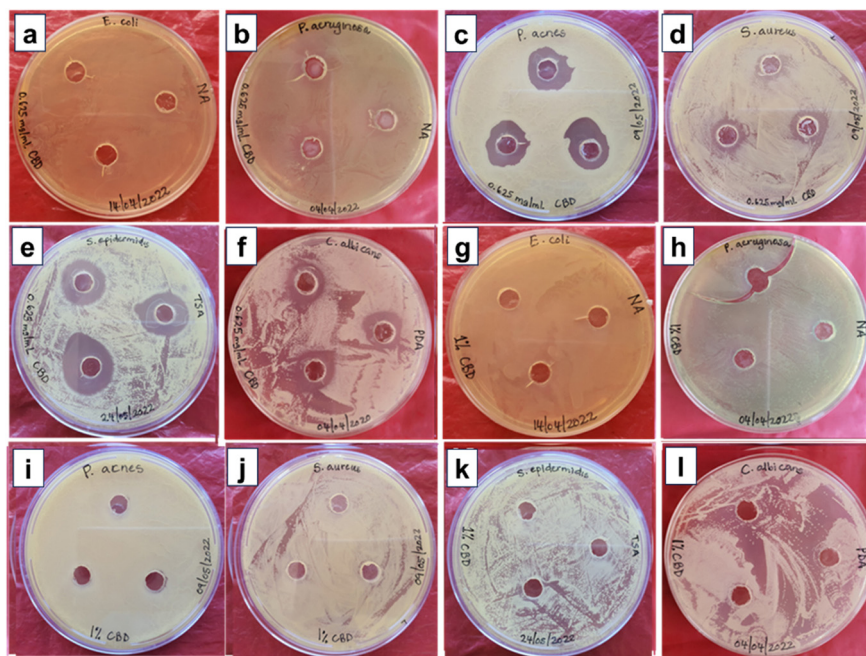


Fig. 8 Antimicrobial activity evaluation using the agar well diffusion method. CBD-IS-D against (a) *E. coli*, (b) *P. aeruginosa*, (c) *C. acnes* (d) *S. aureus*, (e) *S. epidermidis*, (f) *C. albicans* and CBD-W against (g) *E. coli*, (h) *P. aeruginosa*, (i) *C. acnes* (j) *S. aureus*, (k) *S. epidermidis*, (l) *C. albicans*.

Table 4 MICs of CBD-IS-D against selected microorganisms

Microorganism	Type	MIC ($\mu\text{g mL}^{-1}$)
<i>S. aureus</i>	Bacteria (Gram-positive)	156.25
<i>S. epidermidis</i>	Bacteria (Gram-positive)	2.44
<i>C. acnes</i>	Bacteria (Gram-positive)	2.44
<i>C. albicans</i>	Fungus	> 312.5
<i>M. furfur</i>	Fugus	312.5

factors that could influence antimicrobial efficacy. While this study reports the observation that CBD exhibited a lack of antimicrobial activity against Gram-negative bacteria, it was also observed to impart significant antimicrobial activity to Gram-positive bacteria. It is also worth noting that there is a recent study that reported the selective antimicrobial activity toward a subset of Gram-negative bacteria for the first time.⁶⁶ The use of CBD as an antimicrobial ingredient for skin care applications is not yet well explored. However, it is famously used for its attractive antioxidant and anti-inflammatory properties in skin care products.⁷¹

CBD has become increasingly popular in various topical preparations, and many CBD-based product forms, such as oils, creams, lotions, serums, and tinctures, are available to the public.⁷² However, research studies are scarce investigating the correlation between dermal/transdermal delivery characteristics, efficacy, toxicity and safety of CBD in topical products. Data and information about the adverse effects of CBD are based on studies concerning its oral administration.⁷¹ Good safety and tolerability concerning oral administration of CBD have been reported extensively,^{73–75} and the risks associated with CBD at therapeutic doses (10–20 mg per kg bw per day) are

considered acceptable.⁷² However, the toxic transformation of CBD in formulations either through destabilization or interactions with other chemical ingredients remains possible in acid conditions,⁷⁶ and the likelihood of such events at the established dermal CBD doses needs to be established based on reliable scientific data. The regulatory landscape around the use of CBD for medical and non-medical purposes is still evolving, and regulatory discrepancies exist across the globe on the dosage range and purity.⁷⁷ Moreover, the physicochemical characteristics of CBD warrant the need for innovative formulation strategies that can enhance its permeation into deeper skin strata,⁷⁸ addressing challenges related to bioavailability, which indicate potential avenues for future research in the understanding of CBD-based product performance, safety and toxicology.

5 Conclusions

This study explored CBD's stability and functional properties for prospective application in topical formulations. The central concept of the research design was to develop a fundamental understanding of the biological and physicochemical characteristics of the ingredient that can be scientifically validated for the development of various topical products. Regarding the structural stability of solubilized CBD, it was observed that the solvent or the solubilizing medium used significantly influenced the structural integrity; ethanolic solutions were more stable than aqueous solutions. Discolouration and degradation were observed for CBD solutions not stored under dark conditions, high temperatures, and acidic/basic conditions. From a formulation processing point of view, this would mean the



low-temperature addition of CBD (below 40 °C at the final stage of processing) and maintaining a neutral pH for the formulations containing CBD is necessary. As CBD exist in a surfactant-rich environment in the product formulation, storage under refrigeration conditions would ensure CBD stability and product efficacy. The findings of this study also suggested that CBD in powder form was structurally stable, allowing room-temperature (≤ 25 °C) storage of the ingredient, preferably in dark conditions. Antioxidant and anti-collagenase properties suggest prospects of CBD in sunscreen products (as ROS scavengers) and as an antioxidant additive in formulations to improve the stability of other active ingredients. The antimicrobial properties of CBD against Gram-positive bacterial and fungal species suggest opportunities for CBD to be an active ingredient in antimicrobial products such as anti-acne, anti-dandruff, and deodorants. The poor activity observed for the aqueous solution of CBD, however, indicates that the presence of emulsifiers and other ingredients may alter the efficacy of CBD in the formulation. There is also a strong need to establish CBD's efficacy and safe dosage limit in formulations by combining skin penetration studies, *in vitro* toxicity, and *in vivo* skin safety studies.

Data availability statement

The data that support the findings of this study are available from the corresponding author upon reasonable request.

Author contributions

Sreejarani Kesavan Pillai: conceptualization, data curation, formal analysis, funding acquisition, investigation, methodology, project administration, writing – original draft. Nazia Hassan Kera: data curation, formal analysis, writing – review & editing. Phumelele Kleyi: data curation, formal analysis, writing – review & editing. Marinda de Beer: data curation, formal analysis, writing – review & editing. Matin Magwaza: resources and analysis of CBD. Suprakas Sinha Ray: funding acquisition, writing – review & editing.

Conflicts of interest

The authors declare no conflict of interest.

Acknowledgements

Researchers in this project team wish to acknowledge Tautomer Biosciences Pty Ltd, for the research collaboration (C5EEM08) and material (CBD) supply. The project team is also thankful to the Department of Science and Innovation (DSI) (C6E0085), Council for Scientific and Industrial Research (CSIR) (C1E0080), and Centre for Nanostructures and Advanced Materials (CeNAM) for the laboratory and characterization facilities.

References

- 1 L. R. M. Eagleston, N. K. Kalani, R. R. Patel, H. K. Flaten, C. A. Dunnick and R. P. Dellavalle, *Dermatol. Online J.*, 2018, **24**, 13030–13047.
- 2 E. Papaseit, C. Pérez-Mañá, A. P. Pérez-Acevedo, O. Hladun, M. C. Torres-Moreno, R. Muga, M. Torrens and M. Farré, *Int. J. Med. Sci.*, 2018, **15**, 1286–1295.
- 3 N. Jhawar, E. Schoenberg, J. V. Wang and N. Saedi, *Clin. Dermatol.*, 2019, **37**, 279–281.
- 4 K. M. Nelson, J. Bisson, G. Singh, J. G. Graham, S.-N. Chen, J. B. Friesen, J. L. Dahlin, M. Niemitz, M. A. Walters and G. F. Pauli, *J. Med. Chem.*, 2020, **63**, 12137–12155.
- 5 C. Mazzetti, E. Ferri, M. Pozzi and M. Labra, *Sci. Rep.*, 2020, **10**, 3697–3703.
- 6 I. G. Trofin, G. Dabija, D. Vaireanu and L. Filipescu, *Rev. Chim.*, 2012, **63**, 422–427.
- 7 Y. Gaoni and R. Mechoulam, *Tetrahedron*, 1966, **22**, 1481–1488.
- 8 R. Abu-Sawwa and C. Stehling, *J. Pediatr. Pharmacol. Ther.*, 2020, **25**, 75–77.
- 9 P. W. Hashim, J. L. Cohen, D. T. Pompei and G. Goldenberg, *Cutis*, 2017, **100**, 50–52.
- 10 T. Bíró, B. I. Tóth, G. Haskó, R. Paus and P. Pacher, *Trends Pharmacol. Sci.*, 2009, **30**, 411–420.
- 11 A. Oláh, B. I. Tóth, I. Borbíró, K. Sugawara, A. G. Szöllösi, G. Czifra, B. Pál, L. Ambrus, J. Kloepper and E. Camera, *J. Clin. Invest.*, 2014, **124**, 3713–3724.
- 12 A. Wroński, I. Jarocka-Karpowicz, A. Stasiewicz and E. Skrzydlewska, *Molecules*, 2023, **28**, 1192–1213.
- 13 N. Jordan, J. Zakrajšek, S. Bohanec, R. Roškar and I. Grabnar, *Drug Dev. Ind. Pharm.*, 2018, **44**, 778–786.
- 14 R. Mechoulam and L. Hanuš, *Chem. Phys. Lipids*, 2002, **121**, 35–43.
- 15 K. B. Scheidweiler, M. Andersson, M. J. Swortwood, C. Sempio and M. A. Huestis, *Drug Test. Anal.*, 2017, **9**, 143–147.
- 16 R. Pacifici, E. Marchei, F. Salvatore, L. Guandalini, F. P. Busardò and S. Pichini, *Clin. Chem. Lab. Med.*, 2017, **55**, 1555–1563.
- 17 E. J. Mavundza, T. E. Tshikalange, N. Lall, A. A. Hussein, F. N. Mudau and J. J. M. Meyer, *J. Med. Plants Res.*, 2010, **4**, 2584–2587.
- 18 N. Lall, A. B. Van Staden, S. Rademan, I. Lambrechts, M. N. De Canha, J. Mahore, S. Winterboer and D. Twilley, *S. Afr. J. Bot.*, 2019, **126**, 241–249.
- 19 F. Chen, G. Du, M. Shih, H. Yuan, P. Bao, S. Shi, Y. Cang and Z. Zhang, *PLoS One*, 2019, **14**, 227202.
- 20 K. N. Yoon and T. S. Lee, *J. Mushroom*, 2021, **19**, 150–159.
- 21 E. G. Andriotis, P.-K. Monou, A. Louka, E. Papaefstathiou, G. K. Eleftheriadis and D. G. Fatouros, *Drug Dev. Ind. Pharm.*, 2020, **46**, 1569–1577.
- 22 R.-A. Vlad, T. Sovany, K. Kristó, Y. Ibrahim, A. Ciurba, Z. Aigner, D. L. Muntean and G. Regdon, *Farm*, 2021, **69**, 426–433.
- 23 R.-A. Vlad, P. Antonoaea, N. Todoran, D.-L. Muntean, E. M. Rédei, O. A. Silasi, A. Tătaru, M. Birsan, S. Imre and A. Ciurba, *Saudi Pharm. J.*, 2021, **29**, 1029–1042.



- 24 P. Lv, D. Zhang, M. Guo, J. Liu, X. Chen, R. Guo, Y. Xu, Q. Zhang, Y. Liu and H. Guo, *J. Drug Delivery Sci. Technol.*, 2019, **51**, 337–344.
- 25 A. J. Josiah, S. K. Pillai, W. Cordier, M. Nell, D. Twilley, N. Lall and S. S. Ray, *ACS Omega*, 2021, **6**, 29078–29090.
- 26 N. Geskovski, G. Stefkov, O. Gigopulu, S. Stefov, C. W. Huck and P. Makreski, *Spectrochim. Acta, Part A*, 2021, **251**, 119422.
- 27 E. Kosović, D. Sýkora and M. Kuchař, *Pharmaceutics*, 2021, **13**, 412–422.
- 28 R. K. Ameta, K. Soni and A. Bhattarai, *CColloids Interfaces*, 2023, **7**, 16–37.
- 29 T. Schmidt, J. Stommel, T. Kohlmann, A. E. Kramell and R. Csuk, *Results Chem.*, 2021, **3**, 100234.
- 30 R. C. Wheast, *Handbook of Chemistry and Physics*, CRC Press, Boca Raton, 1983.
- 31 J. Vacek, J. Vostalova, B. Papouskova, D. Skarupova, M. Kos, M. Kabelac and J. Storch, *Free Radical Biol. Med.*, 2021, **164**, 258–270.
- 32 R. Mechoulam, L. O. Hanuš, R. Pertwee and A. C. Howlett, *Nat. Rev. Neurosci.*, 2014, **15**, 757–764.
- 33 P. G. Jones, L. Falvello, O. Kennard, G. M. Sheldrick and R. Mechoulam, *Acta Crystallogr., Sect. B: Struct. Crystallogr. Cryst. Chem.*, 1977, **33**, 3211–3214.
- 34 A. I. Fraguas-Sánchez, A. Fernández-Carballido, C. Martin-Sabroso and A. I. Torres-Suárez, *J. Chromatogr. B: Anal. Technol. Biomed. Life Sci.*, 2020, **1150**, 122188.
- 35 Y. A. Tan, S. H. Ong, K. G. Berger, H. H. Oon and B. L. Poh, *J. Am. Oil Chem. Soc.*, 1985, **62**, 999–1006.
- 36 J. W. Fairbairn, J. A. Liebmann and M. G. Rowan, *J. Pharm. Pharmacol.*, 1976, **28**, 1–7.
- 37 C. E. Turner and J. T. Henry, *J. Pharm. Sci.*, 1975, **64**, 357–359.
- 38 D. Löf D, K. Schillén and L. Nilsson, *J. Food Sci.*, 2011, **76**, 35–39.
- 39 R. D. Kirk, T. Akanji, H. Li, J. Shen, S. Allababidi, N. P. Seeram, M. J. Berlin and H. Ma, *Med. Uses Cannabis Cannabinoids*, 2022, **5**, 129–137.
- 40 O. V. Zillich, U. Schweiggert-Weisz, P. Eisner and M. Kerscher, *Int. J. Cosmet. Sci.*, 2015, **37**, 455–464.
- 41 V. M. Di Mambro and M. J. V. Fonseca, *J. Pharm. Biomed. Anal.*, 2005, **37**, 287–295.
- 42 C. Le Bourvellec and C. Renard, *Crit. Rev. Food Sci.*, 2012, **52**, 213–248.
- 43 C. D. Di Mattia, G. Sacchetti, D. Mastrocola, D. K. Sarker and P. Pittia, *Food Hydrocolloids*, 2010, **24**, 652–658.
- 44 J. Deng, W. Cheng and G. Yang, *Food Chem.*, 2011, **125**, 1430–1435.
- 45 M. Kitamura, Y. Kiba, R. Suzuki, N. Tomida, A. Uwaya, F. Isami and S. Deng, *Medicines*, 2020, **7**, 57–63.
- 46 C. Russo, M. Lavorgna, R. Nugnes, E. Orlo and M. Isidori, *Sci. Rep.*, 2021, **11**, 22494–22507.
- 47 M. Tura, M. Mandrioli and T. Gallina Toschi, *Molecules*, 2019, **24**, 3485–3500.
- 48 A. J. Hampson, M. Grimaldi, J. Axelrod and D. Wink, *Proc. Natl. Acad. Sci. U. S. A.*, 1998, **95**, 8268–8273.
- 49 H. Boulebd, D. M. Pereira, I. A. Khodja, N. T. Hoa, A. Mechler and Q. V. Vo, *J. Mol. Liq.*, 2022, **346**, 118277.
- 50 H. Boulebd, A. Mechler, N. T. Hoa, P. C. Nam, D. T. Quang and Q. V. Vo, *New J. Chem.*, 2021, **45**, 7774–7780.
- 51 M. B. Davies, J. Austin and D. A. Partridge, *Vitamin C: its chemistry and biochemistry*, Royal society of chemistry, 1991.
- 52 S. D. Gupta and S. K. Masakapalli, *Chin. J. Nat. Med.*, 2013, **11**, 616–620.
- 53 S. Parvez, M. Kang, H. Chung and H. Bae, *Phyther. Res.*, 2007, **21**, 805–816.
- 54 A. Manosroi, C. Chankhampan, B. O. Kietthanakorn, W. Ruksiriwanich, P. Chaikul, K. Boonpisuttinant, M. Sainakham, W. Manosroi, T. Tangjai and J. Manosroi, *Chiang Mai J. Sci.*, 2019, **46**, 180–195.
- 55 S. Goenka, *J. Xenobiot.*, 2022, **12**, 131–144.
- 56 Y. S. Hwang, Y.-J. Kim, M. O. Kim, M. Kang, S. W. Oh, Y. H. Nho, S.-H. Park and J. Lee, *Chem. – Biol. Interact.*, 2017, **273**, 107–114.
- 57 Y. Y. Kao, T. F. Chuang, S. H. Chao, J. H. Yang, Y. C. Lin and H. Y. Huang, *J. Tradit. Complementary Med.*, 2013, **3**, 163–170.
- 58 V. N. Sumantran, A. A. Kulkarni, A. Harsulkar, A. Wele, S. J. Koppikar, R. Chandwaskar, V. Gaire, M. Dalvi and U. V. Wagh, *J. Biosci.*, 2007, **32**, 755–761.
- 59 M. Zagórska-Dziok, T. Bujak, A. Ziemlewska and Z. Nizioł-Łukaszewska, *Molecules*, 2021, **26**, 802–822.
- 60 A. Gęgotek, S. Atalay, A. Wroński, A. Markowska and E. Skrzydlewska, *Oxid. Med. Cell. Longevity*, 2021, **2021**, 7624389.
- 61 R. Ramer, J. Merkord, H. Rohde and B. Hinz, *Biochem. Pharmacol.*, 2010, **79**, 955–966.
- 62 S. Y. Rawal, M. K. Dabbous and D. A. Tipton, *J. Periodontal Res.*, 2012, **47**, 320–329.
- 63 L. Schofs, M. D. Sparo and S. F. Sanchez Bruni, *Pharmacol. Res. Perspect.*, 2021, **9**, 761–784.
- 64 J. R. Borchardt, D. L. Wyse, C. C. Sheaffer, K. L. Kauppi, R. G. Fulcher, N. J. Ehlke, D. D. Biesboer and R. F. Bey, *J. Med. Plants Res.*, 2008, **2**, 98–110.
- 65 S. Kaur, C. Sharma, S. Chaudhry and R. Aman, *Res. J. Microbiol.*, 2015, **10**, 280–287.
- 66 M. A. T. Blaskovich, A. M. Kavanagh, A. G. Elliott, B. Zhang, S. Ramu, M. Amado, G. J. Lowe, A. O. Hinton, D. M. T. Pham and J. Zuegg, *Commun. Biol.*, 2021, **4**, 1–18.
- 67 C. S. Wassmann, P. Højrup and J. K. Klitgaard, *Sci. Rep.*, 2020, **10**, 4112–4123.
- 68 S. Frassinetti, M. Gabriele, E. Moccia, V. Longo and D. Di Gioia, *LWT–Food Sci. Technol.*, 2020, **124**, 109149.
- 69 L. D. Martinenghi, R. Jönsson, T. Lund and H. Jenssen, *Biomolecules*, 2020, **10**, 900–915.
- 70 G. Zengin, L. Menghini, A. Di Sotto, R. Mancinelli, F. Sisto, S. Carradori, S. Cesa, C. Frascchetti, A. Filippi and L. Angiolella, *Molecules*, 2018, **23**, 3266–3292.
- 71 B. P. Ferreira, G. Costa, F. Mascarenhas-Melo, P. C. Pires, F. Heidarizadeh, P. S. Giram, P. G. Mazzola, C. Cabral,



- F. Veiga and A. C. Paiva-Santos, *Phytochem. Rev.*, 2023, **22**, 781–828.
- 72 J. Li, R. Carvajal, L. Bruner and N. E. Kaminski, *Food Chem. Toxicol.*, 2021, **157**, 112600.
- 73 O. Devinsky, R. Nabbout, I. Miller, L. Laux, M. Zolnowska, S. Wright and C. Roberts, *Epilepsia*, 2019, **60**, 294–302.
- 74 L. C. Laux, E. M. Bebin, D. Checketts, M. Chez, R. Flamini, E. D. Marsh, I. Miller, K. Nichol, Y. Park, E. Segal, L. Seltzer, J. P. Szaflarski, E. A. Thiele and A. Weinstock, *Epilepsy Res.*, 2019, **154**, 13–20.
- 75 A. Herlopian, E. J. Hess, J. Barnett, A. L. Geffrey, S. F. Pollack, L. Skirvin, P. Bruno, J. Sourbron and E. A. Thiele, *Epilepsy Behav.*, 2020, **106**, 106988.
- 76 P. Golombek, M. Müller, I. Barthlott, C. Sproll and D. W. Lachenmeier, *Toxics*, 2020, **8**, 41–61.
- 77 J. P. Liebling, N. J. Clarkson, B. W. Gibbs, A. S. Yates and S. E. O'Sullivan, *Cannabis Cannabinoid Res.*, 2022, **7**, 207–213.
- 78 A. O. Tijani, D. Thakur, D. Mishra, D. Frempong, U. I. Chukwunyere and A. Puri, *J. Controlled Release*, 2021, **334**, 427–451.

